JOURNAL OF GUIDANCE, CONTROL, AND DYNAMICS
Vol. 16, No. 5, September–October 1993

Piezoelectric Actuator Design for Vibration Suppression: Placement and Sizing

Santosh Devasia,* Tesfay Meressi,* Brad Paden,† and Eduardo Bayo†
University of California, Santa Barbara, Santa Barbara, California 93106

In this paper we consider the problem of simultaneous placement and sizing of distributed piezoelectric actuators to achieve the control objective of damping vibrations in a uniform beam. For several closed-loop performance measures we obtain optimal placement and sizing of the actuators using a simple numerical search algorithm. These measures are applied to the specific example of a simply-supported beam with piezoelectric actuators, and their relative effectiveness is discussed. We demonstrate that the controllability grammian is not suitable to determine actuator placement for vibration suppression problems.

Nomenclature

A_b = cross-sectional area of the beam
b = cross-sectional width
C_p = capacitance of the piezoelectric actuator
d_{31} = piezoelectric constant
E_a = Young's modulus of the adhesive layer
E_b = Young's modulus of the beam column
E_p = Young's modulus of the piezoactuator
g_{31} = strain to voltage constant
I_b = area moment of inertia of the beam
I_{Eq} = equivalent area moment of inertia
t_a = thickness of the adhesive layer
t_b = thickness of the beam column
t_p = thickness of the piezoactuator
v_1 = voltage applied to the top piezo
v_2 = voltage applied to the bottom piezo
$y(x)$ = vertical displacement of the neutral axis
δ' = derivative of the delta function
ρ_b = density of the beam

I. Introduction

THE control of large flexible structures has been considered for some time.[1,2] However, the recent application of piezoelectric materials by Crawley[3] and Bailey and Hubbard[4] for actuation of flexible structures has added new dimensions to the control problem. This comes from the fact that these actuators can be distributed along structural members for vibration and shape control. In this paper we consider the problem of simultaneous *placement* and *sizing* of distributed piezoelectric actuators to achieve the control objective of damping vibrations in a uniform beam.

Figure 1 shows a specific example of a simply-supported beam with piezoelectric actuator strips attached to both sides. Our goal is to find the position and length of piezoelectric actuators to maximize modal damping when feedback control is applied. In contrast to previous approaches, we simultaneously optimize the position and length of the actuator strips. For several *closed-loop* performance measures we obtain optimal placement and sizing of the actuators using a simple numerical search algorithm.

In Crawley's early work the actuator was simply placed with one bending mode in mind at the location of maximum strain for that mode.[3] However the placement problem for the case with two or more controlled modes was not addressed. Kondoh et al.[5] used the linear quadratic-optimal control framework to perform sensor and actuator placement, but formulated the problem such that the solution is initial condition dependent—this dependence is removed here. Controllability was used as a performance measure for placement of a point actuator in Refs. 6 and 7. These methods are shown to yield less effective results for vibration damping in beams than those based on closed-loop performance measures. Previous works on actuator placement have not dealt with the sizing problem. We incorporate this as an additional optimization parameter and show that increasing the size of the actuator is not necessarily better.

Questions of robustness to spillover and actuator dynamics have been raised and addressed in Refs. 1, 2, and 8, but are not addressed here. Another important issue is the problems involved in the implementation of controllers for the distributed piezoactuators. These include depoling, nonlinearity, hysteresis, and creep effects in the actuator.[9] Depoling may be avoided by maintaining the applied field below the coercive field. Within the depoling limits, the nonlinearity between the applied electric field and the resulting actuation strain may require the use of more complex models.[10] An alternative is the linearization of this relationship about the operating point.[11] Creep and strain rate dependence of the actuator become important at large strains and low frequencies. Hysteresis also plays an important role at low frequencies. Significant performance improvement over such behavior is possible by commanding the induced charge rather than the voltage applied to the actuator.[12] Other related issues due to actuator dynamics are considered in Refs. 13 and 14, but not addressed in this paper. We note, however, that piezoactuators have fast dynamics relative to electromagnetic actuators and are attractive in this regard.

The remainder of the paper is organized in the following format. In Sec. II a state-space model of a piezoelectric actuated beam of finite length is derived. Section III formulates the placement problem with respect to three performance cri-

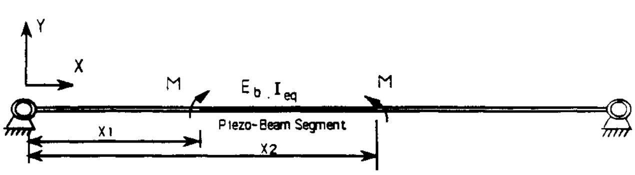

Fig. 1 Simply-supported beam.

Received April 13, 1992; revision received Nov. 6, 1992; accepted for publication Nov. 14, 1992.

*Research Assistant, Department of Mechanical and Environmental Engineering.

†Associate Professor, Department of Mechanical and Environmental Engineering.

teria. These are applied to the simply-supported beam in Sec. IV and compared. Our conclusions are made in Sec. V. The Appendix contains detailed calculations of the mechanics of a piezoactuated beam.

II. State-Space Model of Actuated Beam

In this section we develop a state-space model for the transverse vibrations of the finite beam. The boundary conditions are any combination of pinned, clamped, or free. A pair of piezos attached to the top side and bottom side of the beam is used to actuate the beam as shown in Fig. 2. A second pair is used as sensors. Collocation is achieved since the two pairs are located side by side. The input to the system is the voltage v applied to the actuator pair and the output is the strain-induced voltage generated by the sensors. We show in the Appendix that the net forcing of the beam is equivalent to two equal and opposite moments, M and $-M$ (Fig. 3), applied to the beam at the piezo endpoints x_1 and x_2. Moreover, the moment M is proportional to the input voltage

$$M = Kv \tag{1}$$

The partial differential equation describing the distributed parameter system is therefore

$$E_b I_b y'''' + \rho_b A_b \ddot{y} = M\left[\delta'(x-x_2) - \delta'(x-x_1)\right] \tag{2}$$

We assume that the effects of the actuator on the mode shapes are negligible, which is valid if the dimensions of the piezo are small compared with those of the beam. This formulation is simple and is sufficient for the work presented in this paper. More detailed models are available in Ref. 9. Our assumption of a finite beam with pinned, clamped, or free boundary conditions guarantees a modal decomposition of the form

$$y(x,t) = \sum_{i=1}^{\infty} \Phi_i(x)\eta_i(t) \tag{3}$$

where the $\Phi_i(x)$ are the normalized orthogonal mode shapes and the $\eta_i(t)$ are the modal amplitudes. Substituting Eqs. (1) and (3) into (2) and projecting onto the ith mode yields decoupled modal equations

$$\rho_b A_b \ddot{\eta}_i(t) + E_b I_b \psi_i \eta_i(t) = \left[\Phi_i'(x_2) - \Phi_i'(x_1)\right] K v(t) \tag{4}$$

where ψ_i determines the modal stiffness and is given by

$$\psi_i \triangleq \int_0^{L_b} \Phi_i \cdot \Phi_i'''' \, \mathrm{d}x \tag{5}$$

Define

$$\omega_i^2 \triangleq \frac{E_b I_b \psi_i}{\rho_b A_b} \quad \text{and} \quad B_i \triangleq \frac{1}{\rho_b A_b}\left[\Phi_i'(x_2) - \Phi_i'(x_1)\right] K \tag{6}$$

Then equation (4) can be written as

$$\ddot{\eta}_i(t) + \omega_i^2 \eta_i(t) = B_i v(t) \tag{7}$$

It is clear from Eq. (7) that the ith mode is controllable if and only if B_i is nonzero. In this paper we are trying to control multiple modes with a single piezo and so there must be a compromise placement and sizing such that B_i for each controlled mode is nonzero.

With the sensor placed as shown in Fig. 2, the output of the sensor piezos is a linear combination of the modal amplitudes. Substituting Eq. (3) into Eq. (A9) of the Appendix yields

$$V_s(t) = K_s \sum_{i=1}^{\infty} \eta_i(t)\left[\Phi_i'(x_2) - \Phi_i'(x_1)\right] \tag{8}$$

Define C_i by

$$C_i \triangleq K_s\left[\Phi_i'(x_2) - \Phi_i'(x_1)\right] \tag{9}$$

then

$$\hat{y}(t) = \sum_{i=1}^{\infty} C_i \eta_i(t) \tag{10}$$

If C_i is nonzero then the ith mode is observable. In our case of collocated sensors and actuators (Fig. 2), the ith mode is observable if and only if it is controllable.

If we truncate our representation to n modes, the dynamics can be written as

$$\dot{z}(t) = \bar{A}z(t) + \bar{B}v(t)$$

$$V_s(t) = \bar{C}z(t) \tag{11}$$

where

$$z \triangleq \left[\eta_1 \quad \eta_2 \quad \cdots \quad \eta_n \quad \dot{\eta}_1 \quad \dot{\eta}_2 \quad \cdots \quad \dot{\eta}_n\right]^T \tag{12}$$

$$\bar{A} \triangleq \begin{bmatrix} O_n & I_n \\ -\Omega^2 & 0_n \end{bmatrix}$$

$$\bar{B} \triangleq \begin{bmatrix} O_{n\times 1} \\ \hat{B} \end{bmatrix} = \begin{bmatrix} O_{n\times 1} \\ B_1 \\ \vdots \\ B_n \end{bmatrix}$$

$$\bar{C} \triangleq \left[\hat{C} \quad O_{1\times n}\right] = \left[C_1 \; C_2 \; \cdots \; C_n \quad O_{1\times n}\right] \tag{13}$$

and $\Omega \triangleq \mathrm{diag}(\omega_i, \ldots, \omega_n)$.

We emphasize the fact that $\bar{B}$ and $\bar{C}$ depend on the piezo position and length through x_1 and x_2.

III. Optimal Placement and Sizing of Piezoactuators

In this section we formulate three optimization problems for determining a good placement and length of the piezoactuator. In words they are the following: 1) subject to the constraint that collocated damping control is used, find the placement and length that maximizes damping uniformly in the modes;

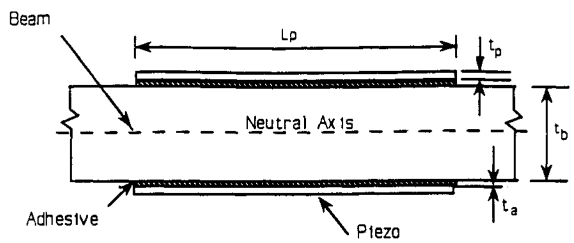

Fig. 2 Beam segment with actuator.

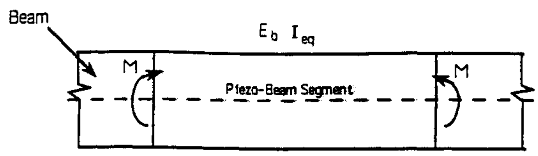

Fig. 3 Equivalent beam segment.

2) assuming the system is detectable and stabilizable, find the placement and length that minimizes a standard linear quadratic cost functional uniformly in initial conditions; and 3) find the placement and length that maximizes the minimum eigenvalue of the controllability grammian (as is done only for the actuator placement problem by Arbel[6]).

Passive Damping Case

For the first optimization problem, we assume a pure collocated damping control given by

$$v(t) = k_d \hat{C} \dot{\eta} \tag{14}$$

where $\eta = [\eta_1 \ \eta_2 \ \cdots \ \eta_n]$ and k_d is the controller gain. With this control, Eq. (11) can be written in vector form as

$$\ddot{\eta} + \Omega^2 \eta = k_d \hat{B} \hat{C} \dot{\eta} \tag{15}$$

and the state-space description becomes

$$\dot{z}(t) = Az(t) \tag{16}$$

where

$$A \triangleq \begin{bmatrix} O_n & I_n \\ -\Omega^2 & -k_d \hat{B}\hat{C} \end{bmatrix} \tag{17}$$

The advantage of such a collocated passive control is that controllers designed for a finite-dimensional model retain the stability of the infinite dimensional plant provided that actuator dynamics can be neglected.[15] Since the bandwidth of a piezo is only limited by its capacitance, actuator dynamics can be justifiably ignored for large space structures. The implementation issues of such controllers have been addressed in Refs. 9 and 14.

We measure the system performance for a particular choice of controller, placement, and piezo length by the rate of decay of system states and therefore seek to place the poles of the system far into the left half of the complex plane. More formally, we perform the following optimization

$$\min_{\substack{L_p \in [0, L_b] \\ X_p \in [L_p/2,\, L_b - L_p/2]}} \ \max_i \ Re \lambda_i(A) \tag{18}$$

where $\lambda_i(A)$ is the ith eigenvalue of A. We vary the length of the piezo L_p from zero to the length of the beam L_b. The piezo mu.t not overlap the ends of the beam hence the center position X_p of the piezo is varied from $L_p/2$ to $L_b - L_p/2$.

Linear Quadratic Regulator Case

The linear quadratic regulator (LQR) is attractive because the controller stabilizes the closed-loop system and also allows for user defined weights on the inputs and states. LQR optimization has been used to reduce the structural vibrations in the control of large flexible structures in Refs. 4 and 7 for a fixed-size actuator. Here we include placement and sizing in the optimization. For the system described by Eq. (11), consider the infinite-horizon time-optimal control problem of minimizing a quadratic cost functional given by

$$J_v \triangleq \int_0^\infty \left[R v(t)^2 + z^T(t) Q z(t) \right] \mathrm{d}t \tag{19}$$

where R is a positive scalar and Q is a positive semidefinite matrix such that the pair $(\bar{A}, Q^{1/2})$ is observable. Provided system (11) satisfies the standard conditions of stabilizability and detectability, the minimum cost $\min_v J_v$ is given by $z^T(t_0) P z(t_0)$, where P is the unique nonnegative-definite solution to the algebraic Riccati equation[16]

$$P\bar{A} + \bar{A}^T P - P\bar{B} R^{-1} \bar{B}^T P + Q = 0 \tag{20}$$

The corresponding control is

$$v(t) = -R^{-1} \bar{B}^T P z(t) \tag{21}$$

We propose minimizing J_v for the worst case initial condition and therefore pose the following optimization for computing X_p and L_p.

$$\min_{\substack{L_p \in [0, L_b] \\ X_p \in [L_p/2,\, L_b - L_p/2]}} \ \max_{\|z_0\| = 1} \ z_0^T P z_0 \qquad z_0 = z(t_0) \tag{22}$$

This method optimizes performance uniformly in initial conditions in contrast to the approach by Kondoh et al.[5] where a solution sensitive to initial conditions is proposed.

Controllability Grammian Method

Finally, we describe a placement procedure based on the controllability grammian proposed by Ref. 6. This method is useful, but has certain disadvantages discussed in the Conclusion. With the inclusion of structural damping the matrix $\bar{A}$ in the state-space description Eq. (11) becomes

$$A_s \triangleq \begin{bmatrix} O_n & I_n \\ -\Omega^2 & -2\zeta\Omega \end{bmatrix} \tag{23}$$

where ζ is the structural damping coefficient. Since A_s is stable, as the final time T tends to infinity, it can be shown that the finite time controllability grammian $W(0,T)$ approaches W, which is the solution of the Lyapunov equation

$$W A_s^T + A_s W + \bar{B}\bar{B}^T = 0 \tag{24}$$

Based on Arbel's method we perform the optimization

$$\max_{\substack{L_p \in [0, L_b] \\ X_p \in [L_p/2,\, L_b - L_p/2]}} \ \min_i \ \lambda_i(W) \tag{25}$$

to maximize the controllability of all the modes. The three approaches discussed here are compared via an example in the next section.

IV. Example: Simply-Supported Beam

Consider the simply-supported actuated beam (Fig. 1) having the following properties.

Beam properties

$\zeta = 0.01 \qquad E_b = 70$ GPa $\qquad L_b = 0.5$ m

$t_b = 0.01$ m $\qquad b = 0.05$ m $\qquad \rho_b = 2500$ Kg/m^3

Piezoactuator-sensor properties

$E_p = 63$ GPa $\qquad L_p \in [0, L_b] \qquad t_p = 2 \times 10^{-4}$ m

$d_{31} = 120 \times 10^{-12}$ m/V $\qquad g_{31} = 10.6 \times 10^{-3}$ Vm/N

$C_p = 35$ pC

Adhesive properties

$E_a = 2.4$ GPa $\qquad L_a = L_p \qquad t_a = 2 \times 10^{-5}$ m

Using the geometric boundary conditions

$$y(0,t) = y(L,t) = y''(0,t) = y''(L,t) = 0 \tag{26}$$

together with Eqs. (2) and (3), we obtain the equation for the ith mode shape normalized so that

$$\int_0^{L_b} \Phi_i^2 \, \mathrm{d}x = 1$$

$$\Phi_i(x) = \sqrt{2/L_b} \, \sin(i\pi x / L_b) \tag{27}$$

Substituting this into Eqs. (5) and (6), we have

$$\omega_i = \frac{i^2\pi^2}{L_b^2}\sqrt{\frac{E_b I_b}{\rho_b A_b}} \tag{28}$$

The ith component of the input vector $\hat{B}$ is obtained from Eqs. (6) and (27) and is given by

$$B_i = \frac{ibt_b^3 K^* \pi}{12\rho_b A_b I_{\text{Eq}} L_b}\sqrt{\frac{2}{L_b}}\left[\cos\left(\frac{i\pi x_2}{L_b}\right) - \cos\left(\frac{i\pi x_1}{L_b}\right)\right] \tag{29}$$

where K^* and I_{Eq} are as defined in the Appendix by equations (A3) and (A4), respectively. The ith component C_i of the output vector $\hat{C}$ is obtained from Eqs. (9) and (27):

$$C_i = \frac{bt_b g_{31}\pi i}{2C_p L_b}\sqrt{\frac{2}{L_b}}\left[\cos\left(\frac{i\pi x_2}{L_b}\right) - \cos\left(\frac{i\pi x_1}{L_b}\right)\right] \tag{30}$$

Note that a necessary condition for observability and controllability of the ith mode is for the term in parentheses in Eq. (30) to be nonzero. From Eq. (29) we see that B_i is large if x_1 and x_2 are chosen to lie near two different nodes of the ith mode separated by an odd number of half cycles of the mode shape (hence a bigger actuator is not necessarily better!). Also the ith ($i > 1$) mode becomes uncontrollable if the center of the piezo coincides with one of its nodes or the piezo length is an integral multiple of $2L_b/i$. For example, if the piezo length L_p is the same as the beam length L_b, then all of the even modes are uncontrollable.

Simulations were performed for each of the optimization schemes discussed in Sec. III applied to the earlier truncated beam model (with the first two modes). A uniform structural damping coefficient of 0.01 is considered for both of the modes. This implies that the system is stable and hence both detectable and stabilizable. For the passive damping case a controller gain $k_d = 1e-6$ was used. In the LQR based design the placement depends on Q, especially if some states are not penalized. However, to uniformly penalize all modes, Q was taken as $I_{4\times4}$. It was observed in the simulations that the optimum placement and sizing did not vary with R. The results presented are for the $R = 1$ case. The variations of the objective function for the passive damping case with 1) the position of the center of the piezo X_p (optimal over all possible actuator lengths) and 2) the length of the piezo L_p (optimal over possible piezo placements) are shown in Fig. 4. Similar simulation results for the LQR and the controllability grammian methods are shown in Figs. 5 and 6, respectively. Note that as the piezo length L_p approaches the beam length L_b, its midpoint is pushed toward $L_p/2$, making the second mode less controllable. Hence the cost increases as L_p tends to L_b and leads to an optimal actuator length less than L_b. The optimal lengths and positions for the three methods are given in Table 1.

To make a comparison between our LQR method and the initial condition dependent methods described in Refs. 3 and 5 we consider the following two different initial conditions $z_1^T = [1\ 0\ 0\ 0]$ and $z_2^T = [0\ 1\ 0\ 0]$, which correspond to unit displacements in the first and the second modes, respectively. The variation of the cost of control over different actuator

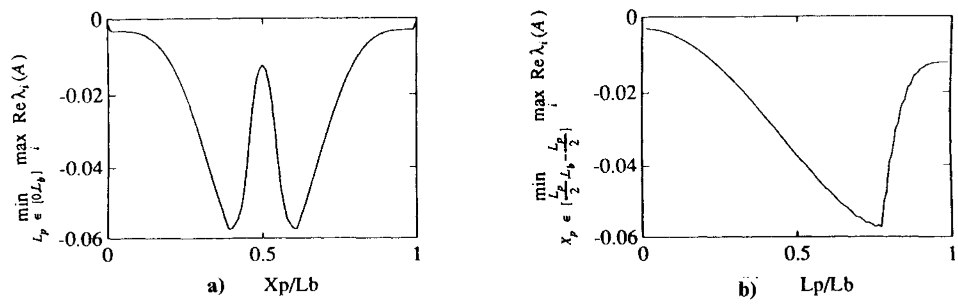

Fig. 4 Passive damping based optimization.

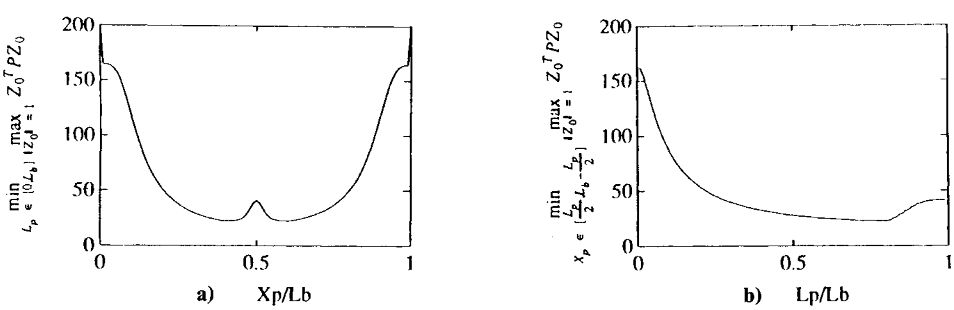

Fig. 5 Linear quadratic regulator based optimization.

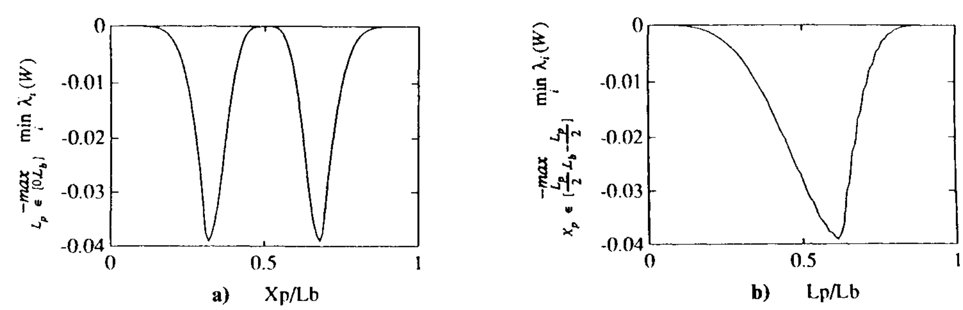

Fig. 6 Controllabilty grammian based optimization.

locations for each of the earlier initial conditions is shown in Fig. 7. The optimization based on these initial conditions results in two different optimum piezo positions at $L_b/2$ and $L_b/4$ suggesting piezo placement at locations where the strain is maximum for the corresponding initial condition. The optimal piezo positions for various initial conditions that are linear combinations of the two modes will vary widely. This problem is easily resolved by the LQR methodology proposed in this paper as it optimizes over all initial conditions.

Next we discuss the controllability grammian method applied by Arbel.[6] The optimized minimum energy control cost for given initial condition $z(t_0)$ and final condition $z(T)$ is equivalent to

$$J \triangleq \left[z(T)-e^{A_s(T-t_0)}z(t_0)\right]' W^{-1}(0,T)\left[z(T)-e^{A_s(T-t_0)}z(t_0)\right] \tag{31}$$

where $e^{A_s(T-t_0)}$ is the state transition matrix.[16] J is the energy required to deviate from the natural motion of the system, which would have reached the state $e^{A_s(T-t_0)}z(t_0)$ at time T without the application of any control. Arbel's method is based on optimizing J (over all possible initial and final conditions) and results in minimizing the maximum eigenvalue of the inverse of the controllability grammian, $W^{-1}(0,T)$, over different actuator positions. However, the control cost J for the finite time regulator problem $[z(T)=0]$ is given by

$$J_r \triangleq \left[e^{A_s(T-t_0)}z(t_0)\right]' W^{-1}(0,T)\left[e^{A_s(T-t_0)}z(t_0)\right] \tag{32}$$

and is not suitably evaluated by Arbel's controllability grammian approach because it fails to consider the effect of $e^{A_s(T-t_0)}$ on J_r in Eq. (32). Next we show that the maximum eigenvalue of $W^{-1}(0,T)$ increases as the system poles move far into the left half of the complex plane. Let γ_i be an eigenvalue of W and let V_i be the corresponding eigenvector such that $\|V_i\|_2=1$. Pre- and post-multiplying the Lyapunov Eq. (24) by V_i^T and V_i, respectively, we obtain

$$V_i^T W A_s^T V_i + V_i^T A_s W V_i + V_i^T \bar{B}\bar{B}^T V_i = 0 \tag{33}$$

Then

$$\gamma_i = -\frac{V_i^T \bar{B}\bar{B}^T V_i}{2V_i^T A_s V_i} \le \frac{|\max_i \lambda_i(\bar{B}\bar{B}^T)|}{\min_i |\lambda_i(A_s)|} \tag{34}$$

This result implies that for a given $\bar{B}$ the eigenvalues of W^{-1} increase if the eigenvalues of A_s move far into the left half plane. Hence Arbel's approach deems the system as less controllable and therefore not desirable even though the shifting of the poles is advantageous for vibration reduction.

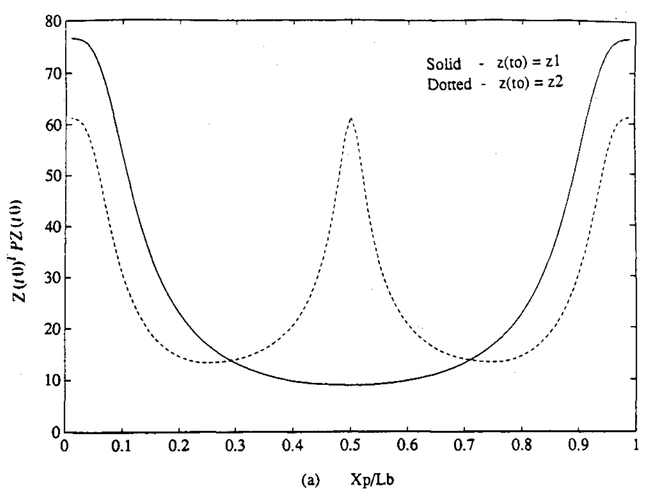

Fig. 7 Initial conditions based optimization.

Table 1 Results

Controller	Optimal $\frac{L_p}{L_b}$	Optimal $\frac{X_p}{L_b}$
Passive	0.7723	0.3961
LQR	0.7921	0.4060
Contr. Gramm.	0.6139	0.3267

This decrease in controllability can be easily illustrated through a scalar example described by

$$\dot{x}(t) = -ax(t) + bu(t) \tag{35}$$

Using Arbel's method, for a large final time T, the eigenvalue of $W(0,T)$ tends to $b^2/2a$, which decreases as a increases, and subsequently the controllability measure deems the system as less controllable even though from a vibration reduction perspective it is more desirable. A similar effect due to the high decay rate in the second mode is seen in the example of the simply-supported beam. The two modes have the same damping coefficient, and so the second mode has a faster decay rate. Arbel's placement method therefore assigns the second mode as less controllable relative to the first mode and hence pushes the placement toward $L_b/4$ where the second mode has maximum strain. Because of a lower decay rate, control of the first mode (which is more controllable when the placement is at the center of the beam) is more critical from a vibration suppression perspective. However, the placement obtained by Arbel's method is further away from the center of the beam and hence results in slower vibration decays in the system as compared to the results obtained through LQR or passive damping methods (Table 1). Thus for vibration reduction, passive damping or LQR based objective functions are more suitable to design the placement of actuators.

V. Conclusion

In this paper we formulated actuator placement and sizing methodologies for vibration suppression in uniform beams. Several closed-loop performance criteria were considered to derive objective functions for optimum placement and sizing of piezoelectric actuators in uniform beams. The paper illustrated through an example that passive damping or linear quadratic regulator based measures are more suitable than the controllability measure for the placement and sizing of actuators to obtain vibration reduction. The procedures developed led to solutions that are independent of initial conditions. The design is also formulated as an eigenvalue problem thereby reducing the required computation considerably.

We also note that the measures proposed in this paper can be applied to any general linear time invariant system and hence the actuator design for vibration suppression can be based on these measures. The question of the existence of optimal designs over different controllers (e.g., all passive controllers) for general linear time invariant systems is the subject of further research.

Appendix: Mechanics of Piezo Actuated Beam

Consider a segment of the piezo beam as shown in Fig. 2. It is assumed for simplicity that the width of the piezo is equal to that of the beam. Using the standard Bernoulli-Euler beam approach, the moment generated by voltage applied to the piezos is given by Ref. 9

$$M^* = bt_pE_p\left[(\Lambda_1-\Lambda_2)(t_b/2+t_a+t_p/2)\right] \tag{A1}$$

where

$$\Lambda_i = \frac{d_{31}v_i}{t_p} \qquad i=1,2 \tag{A2}$$

Thus

$$M^* = bE_p d_{31}(t_b/2 + t_a + t_p/2)(v_1 - v_2) \triangleq K^*(v_1 - v_2)/2 \quad \text{(A3)}$$

M^* is the effective bending moment acting on a beam of equivalent area moment of inertia given by

$$I_{\text{Eq}} = \frac{bt_b^3}{12} + 2\,\frac{b_a t_a^3}{12} + 2b_a t_a\left(\frac{t_b}{2} + \frac{t_a}{2}\right)^2 + 2\,\frac{b_p t_p^3}{12} + 2b_p t_p\left(\frac{t_b}{2} + t_a + \frac{t_p}{2}\right)^2 \quad \text{(A4)}$$

where $b_a = b(E_a/E_b)$ and $b_p = b(E_p/E_b)$ are the equivalent adhesive and piezo widths, respectively. Then the resultant strain of the actuator is

$$\epsilon(x,h) = \frac{M^*(x)h}{E_b I_{\text{Eq}}} \quad \text{(A5)}$$

where x is measured along the length of the piezo and h is the distance from the neutral axis. The previous expression is based on the Bernoulli-Euler model described in Ref. 9 and a detailed explanation of the results based on this model can be found in Ref. 17. If the voltages applied at the top and bottom layers of the piezoactuators are equal in magnitude and opposite in sign ($v_1 = -v_2 \triangleq v$), then equation (A3) becomes $M^* = K^*v$. Without loss of generality one can write the effect of the piezo on the beam as two equal and opposite concentrated moments whose magnitudes are given by $M = Kv$ as shown in Fig. 3, where

$$K \triangleq K^* \frac{bt_b^3}{12 I_{\text{Eq}}} \quad \text{(A6)}$$

The sensor output is obtained as follows. The incremental charge $\mathrm{d}Q$ generated on an infinitesimal area $b\ \mathrm{d}x$ is given by

$$\mathrm{d}Q = g_{31}\,\frac{t_b}{2}\,\frac{d^2y(x)}{\mathrm{d}x^2}\,b\ \mathrm{d}x \quad \text{(A7)}$$

This may be integrated over the sensor covered length of the beam to yield the sensor output voltage

$$V_s(t) = \frac{bt_b g_{31}}{2C_p}\left[y'(x_2,t) - y'(x_1,t)\right] \quad \text{(A8)}$$

$$\triangleq K_s\left[y'(x_2,t) - y'(x_1,t)\right] \quad \text{(A9)}$$

where g_{31} is the strain to voltage constant, C_p is the capacitance and x_1 and x_2 are the locations of the piezo ends.

Acknowledgments

Support from the Air Force Office of Scientific Research through Grant F9620-91-C-0095 and the Astro Aerospace Corporation is gratefully acknowledged.

References

[1]Balas, M. J., "Active Control of Flexible Systems," *Journal of Optimization Theory and Applications,* Vol. 25, No. 3, 1978, pp. 415–436.

[2]Meirovitch, L., and Baruh, H., "Control of Self-Adjoint Distributed-Parameter Systems," *AIAA Journal,* Vol. 5, No. 1, 1980, pp. 60–66.

[3]Crawley, E. F., and De Luis, J., "Use of Piezoelectric Actuators as Elements of Intelligent Structures," *AIAA Journal,* Vol. 25, No. 10, 1985, pp. 1373–1385.

[4]Bailey, T., and Hubbard, J. E., Jr., "Distributed Piezoelectric-Polymer Active Vibration Control of a Cantilever Beam," *Journal of Guidance, Control, and Dynamics,* Vol. 8, No. 5, 1985, pp. 605–611.

[5]Kondoh, S., Yatomi, C., and Koichi, I., "The Positioning of Sensors and Actuators in the Vibration Control of Flexible Systems," *JSME International Journal,* Vol. 33, No. 2, 1990, pp. 145–152.

[6]Arbel, A., "Controllability Measures and Actuator Placement in Oscillatory Systems," *International Journal of Control,* Vol. 33, No. 3, 1981, pp. 565–574.

[7]Fisher, S., "Application of Actuators to Control Beam Flexure in a Large Space Structure," *Journal of Guidance, Control, and Dynamics,* Vol. 12, No. 6, 1989, pp. 874–879.

[8]Goh, C. J., and Caughey, T. K., "On the Stability Problem Caused by Finite Actuator Dynamics in the Collocated Control of Large Space Structures," *International Journal of Control,* Vol. 41, No. 3, 1985, pp. 787–802.

[9]Crawley, E. F., and Anderson, E. H., "Detailed Models of Piezoceramic Actuation of Beams," *Journal of Intelligent Material Systems and Structures,* Vol. 1, No. 1, 1990, pp. 4–25.

[10]Crawley, E. F., and Lazarus, K. B., "Induced Strain Actuation of Isotropic and Anisotropic Plates," AIAA 30th Structural, Structural Dynamics, and Materials Conference, AIAA Paper 89-1326, 1989.

[11]De Luis, J., "Design and Implementation of Optimal Controllers for Intelligent Structures Using Infinite Order Structural Models," Ph.D. Thesis, Massachusetts Inst. of Technology, Cambridge, MA, 1989.

[12]Comstock, R. H., "Charge Control of Piezoelectric Actuators as Elements of Intelligent Structures," U.S. Patent 4,263,527, Draper Laboratories, Cambridge, MA, 1981.

[13]Fanson, J. L., and Garba, J. A., "Experimental Studies of Active Members in Control of Large Space Structures," *Proceedings of the AIAA 29th Structures, Structural Dynamics, and Materials Conference,* AIAA, Washington, DC, 1988, pp. 9–17.

[14]Fanson, J. L., and Caughey, T. K., "Positive Position Feedback Control for Large Space Structures," *AIAA Journal,* Vol. 28, No. 4, 1990, pp. 717–724.

[15]Bhaya, A., and Desoer, C. A., "On the Design of Large Flexible Space Structures (LFSS)," *IEEE Transactions on Automatic Control,* Vol. AC-30, No. 11, 1985, pp. 1118–1120.

[16]Kwakernaak, H., and Sivan, R., *Linear Optimal Control Systems,* Wiley-Interscience, New York, 1972.

[17]Devasia, S., "Modeling of Piezo Electric Actuators," M.S. Thesis, Univ. of California, Santa Barbara, Santa Barbara, CA, 1990.